Research paper

Numerical simulation of the effects of nozzle on thrust performance of rotating detonation engine

Seiichiro Eto*, Yusuke Watanabe*, Nobuyuki Tsuboi*†,
Takayuki Kojima**, and A. Koichi Hayashi***

*Kyushu Institute of Technology, 1−1, Sensui−cho, Tobata−ku, Kitakyushu, Fukuoka, 804−8550, JAPAN
Phone : +81−93−884−3167
†Corresponding author : tsuboi@mech.kyutech.ac.jp

**Aerospace Exploration Agency and Aeronautical Technology Directorate, JAXA,
7−44−1 Jindaiji Higashi−machi, Chofu, Tokyo 182−8522 JAPAN

***Aoyama Gakuin University, 5−10−1, Fuchinobe, Chuo−ku, Sagamihara, Kanagawa 252−5258, JAPAN

Received : November 14, 2014 Accepted : June 10, 2016

Abstract

The effects of the converging-diverging (CD) nozzle on the thrust performance of the rotating detonation engine (RDE) were estimated by using the three-dimensional numerical simulations with the detailed chemical reaction model. The nozzle geometry is based on the reference of Rankin *et al*. The nozzle is composed of the long constant cross section, the short converging section, and the diverging section. The periodic exhaust oscillation is considerably reduced by the present CD nozzle. The pressure difference from the averaged value is approximately 1.2 % and the difference in Mach number is approximately 0.4 %. The increment of I_{sp} using the CD nozzle is approximately 15 s. The nozzle performance is estimated via the thrust coefficient. The thrust coefficient of the CD nozzle used this study is nearly corresponded with the ideal value. The combustion efficiency of C^*, η_{C^*}, are obtained 92-98 % between the combustion chamber pressure of 1.2 and 2.9 MPa.

Keywords : shock wave, detonation engine, numerical simulation

1. Introduction

Detonation is a shock-induced combustion wave propagating through a reactive mixture and it has been investigated for the safety engineering by the past studies. Pulse detonation engine (PDE) is a constant-volume-like combustion engine with a supersonic detonation wave. PDE has recently been recognized as one of new propulsion systems for supersonic transportation. The theoretical thermal efficiency of the detonation engines is known to be better than the conventional constant-pressure combustion engines[1]. PDE provides a better efficiency than the ramjet engines with respect to fuel-based specific impulses (I_{spf}) ; however, the thrust under the low frequency becomes small because of the pulsed flow[1].

Recent researches about propulsion using the detonation are focused on the rotating detonation engine (RDE), which obtains a continuous thrust by using a rotating detonation in a coaxial chamber. The continuous thrust force of RDE is the most notable different from PDE. RDE was first studied by Voiseknovskii[2], and he investigated the spin detonation propagating in the cylinder. Nicholls *et al*.[3] concluded that there are many tasks for the injection of the combustible gas mixture in order to stabilize the rotating detonation. Zhdan *et al*.[4] studied by the experimental and numerical approaches to understand the continuous rotating detonation phenomena and they estimated the suitable length of the combustion chamber. Wolanski *et al*.[5] and Lu *et al*.[6] had also experimentally studied. As for the numerical approach, Hishida *et al*.[7] estimated the detailed shock structure of the rotating detonation. Yi *et al*.[8] simulated RDE with some exhaust nozzles to show the possibility of new propulsive engines. Yamada *et al*.[9] also simulated the

2D RDE to understand the mechanism of transverse wave required for the continuous detonation. Nordeen *et al*.[10] and Schwer et al.[11),12)] simulated RDE in hydrogen/air mixture. Zhou *et al*.[13)] simulated hydrogen/oxygen RDE, however, they did not show the value of I_{sp}. The authors simulated the 3D RDE to show that I_{sp} of RDE is larger than the conventional rocket engine[14)].

Recently, RDE with the nozzle is researched in order to improve the thrust performance. Rankin *et al*.[15)] had experimental study of RDE with the converging-diverging (CD) nozzle to reduce the oscillation in the exhaust flow. This is because the exhaust oscillation is one of the major disadvantages to apply to a gas turbine engine. However, there are many unclear things, such as the details of the flow structure in the internal flow, the effect of the nozzle geometry, and the effects of the mass flow ratio on the thrust performance. In the present study, the 3D simulation for RDE with the CD nozzle is performed to find the effect of nozzle geometry on thrust performance and exhaust oscillation.

2. Computational method

2.1 Numerical methods

The governing equations are the three-dimensional Euler equations with the detail chemical reaction model. The governing equations include 9 species (H_2, O_2, O, H, OH, HO_2, H_2O_2, H_2O, N_2) mass conservation equations. A second-order AUSMDV[16)] is used for numerical flux in the convective terms. In the time integration, the third-order TVD Runge-Kutta method is applied. UT-JAXA[17)] model is used for chemical kinetics to solve the detonation problems. The chemical reaction source terms are treated in a linearly point-implicit manner to avoid the stiffness problem.

2.2 Computational domain

The physical model of RDE is shown in Figure 1. This is a coaxial chamber. 1D detonation results are pasted along the circumferential direction to start the rotating detonation. The computational domain of the 3D simulation is the coaxial chamber attached with the CD nozzle as shown in Figure 2.

There are some boundary condition systems for the mixture injection : the supersonic and subsonic inlets. The supersonic inlet condition is used for most of the simulations because the inlet nozzles for premixed gas typically have a choked condition at the exits of small nozzles. However, many real cases should use a subsonic inlet condition because of the high pressure in the combustion chamber. The subsonic inlet condition is proposed by Zhdan *et al*.[4)].

(1) If the inlet pressure is significantly high, the gas injection is impossible. Side of combustion chamber pressure is assigned the side of nozzle pressure and injection velocity is zero.

(2) If the inlet pressure is high, the gas injects at subsonic without choking. Side of combustion chamber pressure is assigned the side of nozzle pressure.

(3) If the inlet pressure is relatively high, the shock wave occurs in the nozzle and injects at subsonic. Side of combustion chamber pressure is assigned the side of nozzle pressure.

(4) If the inlet pressure is very low, the gas accelerate in expansion region and injects at supersonic. The injection is not affected by the wall pressure. The reactant is injects at supersonic.

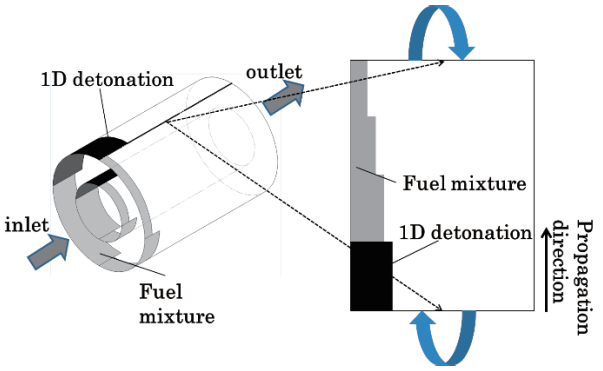

Figure 1 Modeling of 3D RDE.

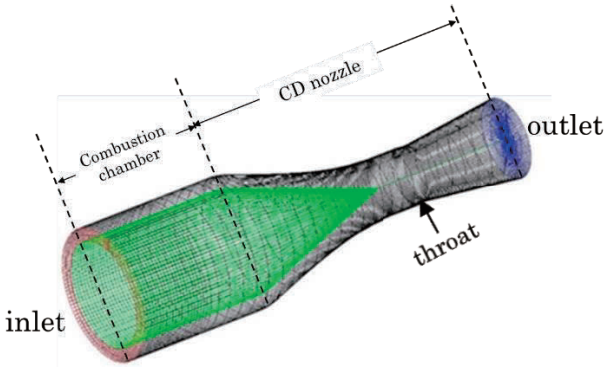

Figure 2 3D grid of RDE with CD nozzle (241x11x601).

The nozzle exit boundary conditions are given at the exit of the RDE by two patterns, but the flow cannot go backwards from the downstream to the upstream :

(1) The exit pressure of the RDE sets the ambient pressure when the exhaust gas velocity is subsonic.

(2) The exit pressure of the RDE is extrapolated from the values in the combustion chamber when the exhaust gas velocity is supersonic.

2.3 Grid system and simulation conditions

The three-dimensional grid system of the RDE with the CD nozzle is shown in Figure 2. The computational grid points are 241(axial) x11(radial) x601(circumferential). The minimum grid widths near the rotating detonation are 5 μm for the axial direction, 9.4 μm for the radial direction, 3.93 and 4.95 μm for the inner and outer circumferential directions, respectively. Therefore, the radius ratio, R_{outer}/R_{inner} is 1.25. The fine grid system is adopted near the rotating detonation head and the coarse grid system is adopted in another region. The nozzle geometry is designed based on the nozzle in the reference of Rankin *et al*.[14)]. The nozzle consists of the long constant cross section area, the short converging section, and the diverging section. In the conical nozzle section, the area ratio of the exit to the throat sets 1.98 to produce supersonic flow with Mach number of approximately 2.2

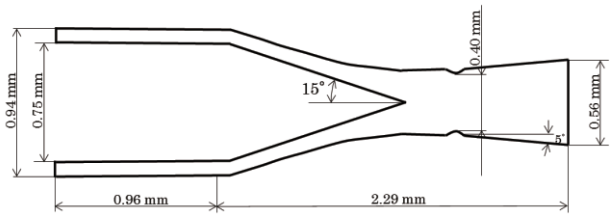

Figure 3 Calculation domain.

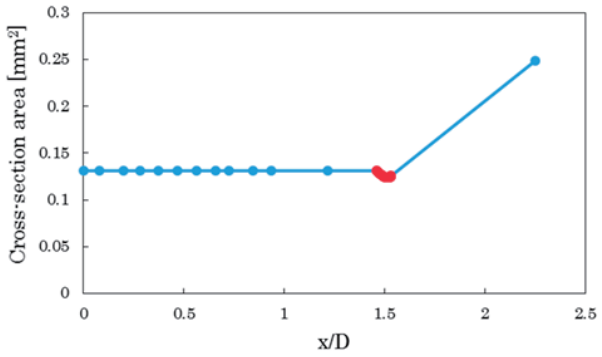

Figure 4 Cross-section area along the axial direction.

under the isentropic condition. Figure 3 shows the detailed calculation domain. The cross section area of the calculation domain along the axial direction is shown in Figure 4.

The ambient conditions behind the nozzle exit are the pressure P_e of 0.01 MPa, the temperature of 300 K. The present simulation conditions in the stagnation chamber are the pressure P_0 of 2-5 MPa. The micro nozzle area ratio of throat to nozzle exit at the port, A^*/A is 0.1. The stoichiometric H_2/O_2 gas mixture is supplied through the micro-nozzles.

3. Results and discussions

3.1 Effects of the nozzle on exhaust oscillation

Figure 5 shows the time history of the averaged pressure on the nozzle exit section. The exhaust oscillation is considerably reduced by the present CD nozzle. The difference from the averaged pressure in the steady state is approximately 0.004 MPa and ratio of the difference to the averaged value (approximately 0.36 MPa) is 1.2 %. The exit Mach number profiles are shown in Figure 6. The difference is approximately 0.008 and ratio of the difference to the averaged value (approximately 1.99) is 0.4 %. This is because the flow is choked at the throat of the CD nozzle. As the above reason, the present CD nozzle has the effect of reducing the exhaust oscillation as shown in Ref. 15.

Figure 7 shows the instantaneous Mach number contours. Figure 8 represents the structure of detonation shock wave in the combustion chamber. Figure 9 (a) and (b) are the cross sections of chamber exit with and without the CD nozzle, respectively. At the chamber exit, the averaged Mach number becomes subsonic with the CD nozzle, however, it becomes supersonic without the CD nozzle. When the CD nozzle is attached, the shock wave disappears at the nozzle exit although the shock wave due to the rotating detonation appears at the chamber exit

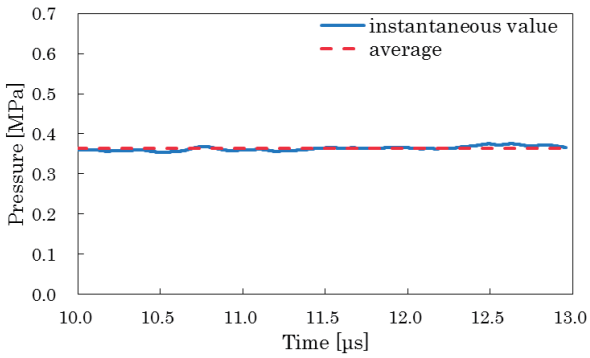

Figure 5 Effect of nozzle on exit pressure.

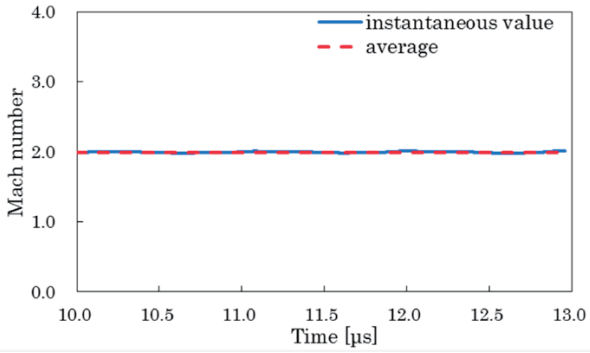

Figure 6 Effect of nozzle on exit Mach number.

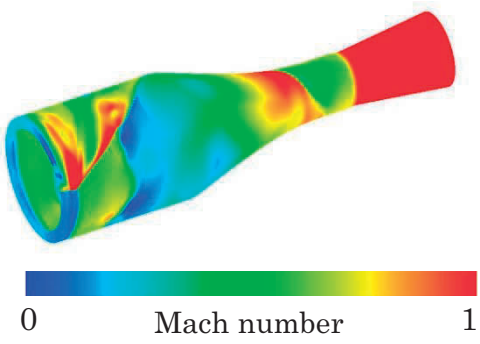

Figure 7 Instantaneous Mach contours of 3D RDE.

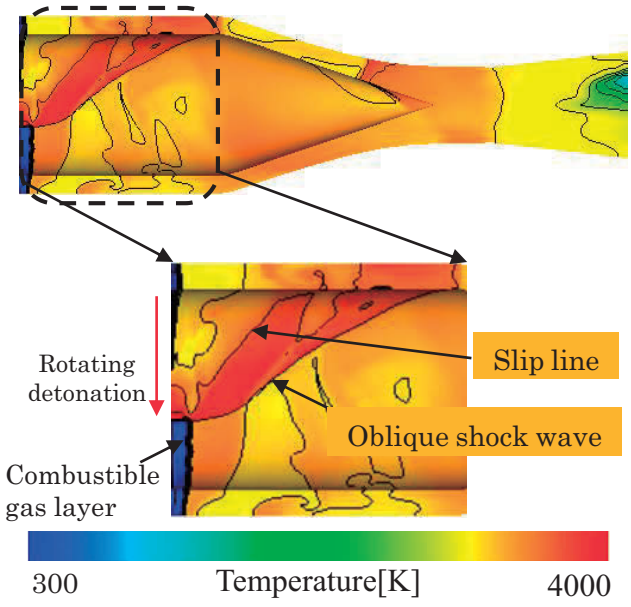

Figure 8 Flow structure in 3D RDE.

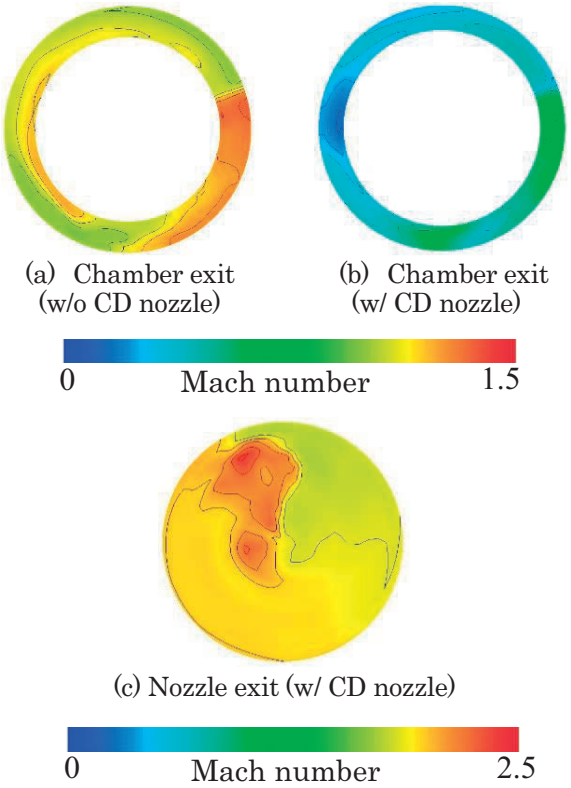

Figure 9 Instantaneous Mach contours at various cross sections.

section in Figure 9 (c).

3.2 Effects of the nozzle on I_{sp}

Table 1 shows the comparison of averaged I_{sp} during five cycles after the steady state of RDE is obtained. Figure 10 shows I_{sp} distribution. The value becomes steady state after 10 μs and calculates as follows :

$$I_{sp} = \frac{F}{g_0 \cdot \dot{m}} \tag{1}$$

Table 1 also includes the calculated I_{sp} for a H_2/O_2 rocket engine with and without the nozzle, assuming a chemical equilibrium state under a vacuum environment. This value is calculated using the Gordon and McBride method[18]. I_{sp} is based on the premixed gas mixture. When the CD nozzle is attached, I_{sp} is improved approximately 15 s. However, I_{sp} for RDE with the CD nozzle is approximately 40 s smaller than I_{sp} for a conventional rocket engine.

3.3 Thrust coefficient C_f and characteristic exhaust velocity C^*

The thrust coefficient C_f is one of the index indicating the nozzle performance. Figure 11 shows the thrust coefficient C_f for P_0 of 2-5 MPa and the comparison with

Table 1 Comparison of I_{sp} between w/o nozzle and w/ nozzle.

	w/o nozzle	w/ nozzle
3D RDE	275.7[s]	289.6[s]
Chemical equilibrium	274.3[s]	328.6[s]

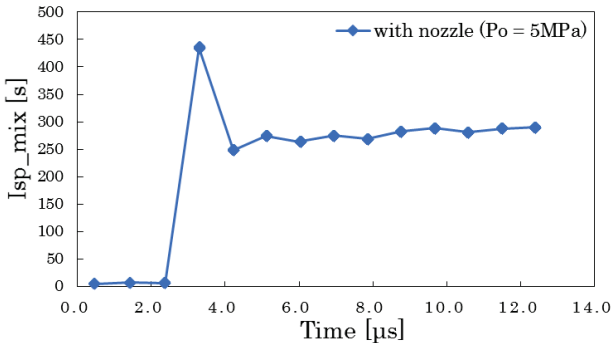

Figure10 I_{sp} versus time.

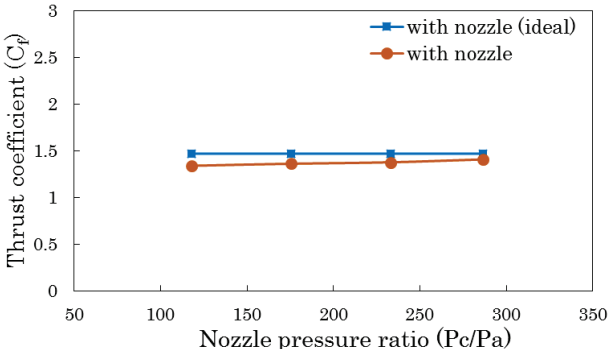

Figure11 Effect of nozzle on thrust coefficient.

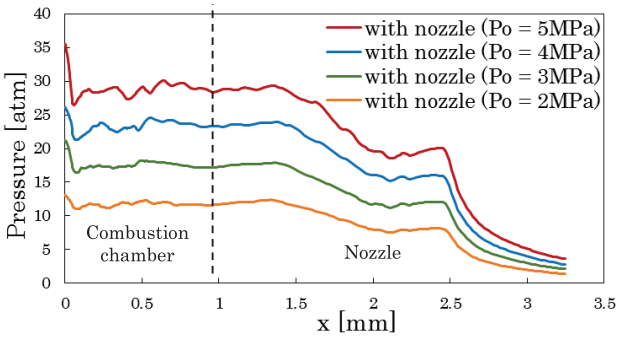

Figure12 Time-averaged pressure distribution along the axial direction.

the ideal value. The ideal value were determined by the Gordon and McBride method[18]. Thrust coefficient C_f was defined as follows :

$$C_f = \frac{F}{P_c \cdot A_t} \tag{2}$$

The time-averaged pressure distributions along the axial direction are shown in Figure 12. P_c is the averaged value at the downstream of the detonation wave in the combustion chamber. It is difficult to define P_c because the value in the combustion chamber of RDE is unsteady. In Figure 11, horizontal axis is the ratio of the combustion chamber pressure P_c to the ambient pressure P_a. This figure indicates the thrust coefficient of the present CD nozzle is nearly corresponded with the ideal value. This nozzle is predicted to exhibit high performance.

The characteristic exhaust velocity C^* is one of the index indicating the combustion chamber performance. C^* was defined as follows :

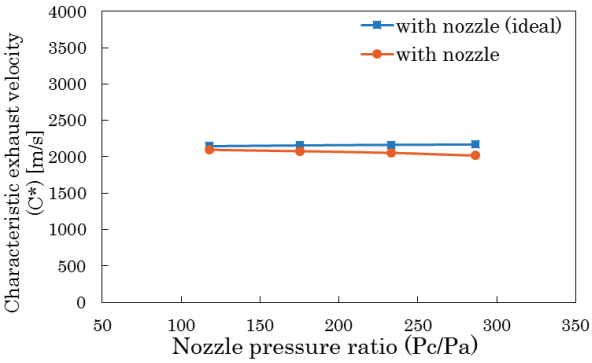

Figure13 Effect of nozzle on characteristic exhaust velocity.

Table 2 Thrust coefficient C_f.

P_c [MPa]	I_{sp} [s]	C_f
1.2	289.85	1.34
1.8	288.02	1.36
2.4	289.89	1.38
2.9	289.82	1.41

Table 3 Combustion efficiency η_{C^*}.

P_c [MPa]	C^*_{RDE} [m/s]	C^*_{ideal} [m/s]	η_{C^*} [%]
1.2	2096.3	2146.5	97.66
1.8	2077.0	2156.9	96.30
2.4	2053.9	2164.5	94.89
2.9	2016.2	2170.0	92.91

$$C^*_{RDE} = \frac{I_{sp} \cdot g_0}{C_f} \tag{3}$$

Table 2 shows the I_{sp} and thrust coefficient for P_c of 1.2-2.9 MPa. Figure 13 shows the characteristic exhaust velocity C^* for P_0 of 2-5 MPa and the comparison with the ideal value determined by the Gordon and McBride method[18]. The values are lower than the ideal value. This is because the energy loss due to the appearance of the shock wave at the upstream of the throat. Combustion efficiency of C^*, η_{C^*}, is shown in Table 3. η_{C^*} was given as follows :

$$\eta_{C^*} = \frac{C^*_{RDE}}{C^*_{ideal}} \times 100 \tag{4}$$

The present results obtains 92-98 % efficiency as compared to the ideal value between $P_c = 1.2$ and 2.9 MPa. The tendency of these values are shown in Figure 14. η_{C^*} decreases as the combustion chamber pressure increases. This is because C^*_{RDE} decreases. The values of I_{sp} are constant for P_c of 1.2-2.9 MPa as shown in Table 2. Therefore, the increases of C_f causes the decreases of C^*_{RDE}. Figure 15 shows the effects of the ratio of the time-averaged thrust to the combustion chamber pressure (F/P_c) on thrust coefficient (C_f). C_f increases as F/P_c increases. C_f is proportional to F/P_c. Therefore, the increases of C_f depends on F. In other words, the decreases of η_{C^*} depends on F increases.

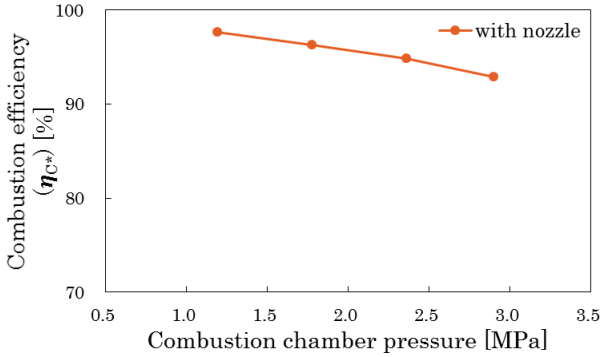

Figure14 Combustion efficiency versus combustion chamber pressure.

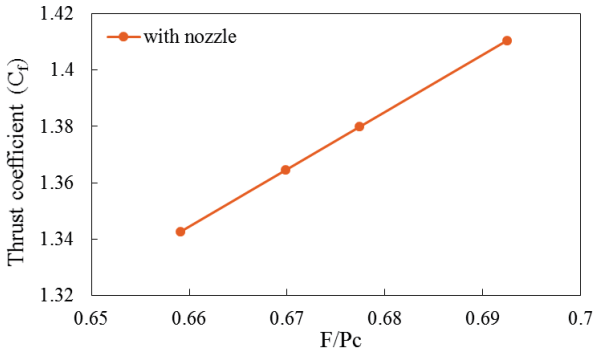

Figure15 Effects of the ratio of the time-averaged thrust to the combustion chamber pressure on thrust coefficient.

4. Conclusions

Three-dimensional numerical analysis of the 3D RDE with the CD nozzle is performed using the detailed chemistry model. The conclusions are as follows :

1) The present CD nozzle reduces the pressure oscillation at the nozzle exit. The amount of the difference of the pressure from the averaged value is approximately 1.2 % and that of Mach number is approximately 0.4 %. At the chamber exit, the averaged Mach number becomes supersonic when the CD nozzle is attached, however, it becomes subsonic for RDE without the CD nozzle.
2) The present CD nozzle affects I_{sp} and the increment is approximately 15 s. The thrust coefficient of the CD nozzle is nearly corresponded with the ideal value. The combustion efficiency of C^* are obtained 92-98 % between $P_c = 1.2$ and 2.9 MPa. It is found that the combustion efficiency of C^* (η_{C^*}) depends on the time-averaged thrust (F).

Acknowledgements

This research was collaborated with Cybermedia Center in Osaka University.

References

1) P.Wolanski, Detonation Propulsion, Proc. Combust. Inst. 34, 125−158 (2013).
2) B.V.Voiteskhovskii, Stationary Detonation, Doklady Akademii Nauk UzSSR, Vol.129, No. 6, pp. 1254−1256 (1959).
3) J.A. Nicholls, R.E.Cullen, and K.W.Ragland, Journal of Spacecraft and Rockets, 3, 893−898 (1966).

4) S.A. Zhdan, F.A. Bykovskii, and E.F. Vedernikov, Combustion, Explosion and Shock Waves, 43, 449−459 (2007).
5) J.Kindaracki, P.Wolanski, and Z. Gut, 22nd International Colloquium on the Dynamics of Explosions and Reactive Systems, Oral 76 (2009).
6) F.K. Lu , N.L. Dunn, and E.M. Braun, 48th AIAA Aerospace Sciences Meeting Including the New Horizons Forum and Aerospace Exposition, AIAA paper 146 (2010).
7) M. Hishida, T. Fujiwara, and P. Worlanski, Shock Waves, 19, 1−10 (2009).
8) T.H.Yi, J. Lou, C. Turangan, B.C. Khoo, and P. Wolanski, 48 th AIAA Aerospace Sciences Meeting Including the New Horizons Forum and Aerospace Exposition, AIAA paper 152 (2010).
9) T. Yamada, A.K Hayashi, E. Yamada, N. Tsuboi, V.E. Tangirala, and T. Fujiwara, Combustion Science and Technology, 182, 1901−1914 (2010).
10) C. A. Nordeen, D. Schwer, F. Schauer, J. Hoke, B. Cetegen, and T. Barber, 49th AIAA Aerospace Sciences Meeting, Orlando, FL, AIAA Paper 0803 (2011).
11) D. A. Schwer and K. Kailasanath, 46th AIAA/ASME/SAE /ASEE Joint Propulsion Conference, Nashville, Tennessee, AIAA Paper 6880 (2010).
12) D. A. Schwer and K. Kailasanath, 49th AIAA Aerospace Sciences Meeting, Orlando, Florida, AIAA Paper 581 (2011).
13) R. Zhou and J.-P. Wang, Combustion and Flame, 159, pp. 3632−3645 (2012).
14) N. Tsuboi, Y. Watanabe, T. Kojima, and A.K. Hayashi, Combustion Institute, Vol. 35, accepted.
15) B.A. Rankin, L.H. John, and R.S. Frederick, 52nd AIAA Aerospace Science Meeting AIAA 2014−1015 (2014).
16) Y. Wada and M. S. Liou, AIAA 83, (1994).
17) K.Shimizu,A.Hibi,M.Koshi,Y. Morii, and N.Tsuboi, Jourmnal of Propulsion and power, 27 383−395 (2011).
18) S. Gordon, J.B. McBride, and J.B., NASA SP273, (1971).